**Article:**
Tantisriyanurak, S., Duguid, H.N., Peattie, L. et al. (2020) Acid functionalized conjugated microporous polymers as a reusable catalyst for biodiesel production. ACS Applied Polymer Materials, 2 (9). pp. 3908-3915. ISSN: 2637-6105

https://doi.org/10.1021/acsapm.0c00595

# Acid functionalized conjugated microporous polymers as a reusable catalyst for biodiesel production

*Supakorn Tantisriyanurak,[a] Harry N. Duguid,[a] Lewis Peattie,[a] and Robert Dawson*[a]*

[a] Department of Chemistry, University of Sheffield S3 7HF, United Kingdom

email: r.dawson@sheffield.ac.uk

A series of conjugated microporous polymers (CMPs) based on bromophenol blue (BB) and bromocresol green (BG) have been synthesized via Sonogashira-Hagihara cross coupling reaction with surface areas up to 747 $m^2/g$. The CMPs can be post functionalized with chlorosulfonic acid to yield corresponding sulfonated polymers with high acidity up to 7.67 mmol/g. The sulfonated CMPs showed excellent catalytic activity for the esterification of free fatty acids and transesterification of various vegetable oils and waste cooking oil as well as excellent reusability up to 4 consecutive runs without significant activity loss. These sulfonated CMPs have potential applications as recyclable acid catalysts for environmentally friendly biodiesel production from waste cooking oil.

Keywords: microporous, porous materials, porous polymers, heterogeneous catalysis, conjugated microporous polymers

## Introduction

Porous organic polymers (POPs), which can be made from organic molecules linked with covalent bonds have been widely researched over the past two decades in various applications such as gas separation, energy storage, sensing and catalysis.[1–7] They can be categorized into two main types based on their structure; those which are crystalline (such as covalent organic frameworks (COFs)[8–10] and a wide variety of amorphous microporous polymers. The vast majority of organic porous polymers belong to the amorphous class which can be further divided into sub-types including hypercrosslinked polymers (HCPs), polymers of intrinsic microporosity (PIMs) and conjugated microporous polymers (CMPs).[1,11,12] CMPs are organic porous organic polymer containing π-conjugated systems with a permanent nanoporous structure leading to high surface areas (typically between 500-1000 $m^2/g$) and high thermal and chemical stability (can be boiled in concentrated acid without loss of porosity). They are typically synthesized using various Group 10 metals with chemistries such as Sonogashira-Hagihara, Suzuki-Miyaura, and Yamamoto couplings.[12–17] Functionalized CMPs have been extensively studied as heterogeneous catalysts due to high efficiency, recyclability and their ability to perform metal free catalysis. CMP networks can be used either as a porous backbone for functional groups with which to perform catalytic reactions i.e. without the use of their extended conjugation, or their extended conjugation can be used to enhance their catalytic activity such as when used as photocatalysts.

Fossil fuel resources are a widely utilized energy source. An increase in demand for energy has resulted in the depletion of non-renewable fossil energy and their emission of high amounts of carbon dioxide and other greenhouse gases is a leading cause of global warming and air pollution.[18] Thus, alternative energy such as solar energy, nuclear power, hydroelectric energy, biomass and biofuel have been considered as cleaner and more sustainable energy sources to overcome these

problems.[19] Plant oils and animal fats are plentiful in nature and have been commonly used in daily life. Cheap vegetable or animal oils or even waste oil can be utilized as a starting material to produce biodiesel.[18,19] According to the UK Department for Transport, biodiesel accounted for 53% of verified renewable fuel and 83% of biodiesel was made from used cooking oil.[20] Wang et al. reported that approximately 5 million tonnes of waste cooking oil were produced in China, so the use of waste oil for biodiesel production not only provides us with clean energy sources but also reduces environmental pollution.[19] Natural oils and fats generally consist of triglycerides and free fatty acids (FFAs) that can be converted to biodiesel such as fatty acid methyl ester (FAME) via transesterification and esterification with methanol, respectively.[18]

Porous polymers derived from both natural and synthetic materials have been widely applied as catalysts for various organic reactions such as selective oxidation[21–24], Sonogashira-Hagihara cross coupling[25], dehydration of fructose to 5-hydroxymethylfurfural (HMF)[26] and biodiesel production[27–36]. Recently, different acid functionalized porous polymers have been synthesized and utilized as catalysts for biodiesel production due to their large surface area, high acidity and excellent thermal and chemical stability.[29–36] For instance, a sulfonated HCP derived from carbazole has previously been prepared by Bhunja et al. and was applied as an acid catalyst for biodiesel production from FFAs at room temperature. The synthesized catalyst exhibited high yield of FAME products and excellent recyclability.[29] Mohan and co-workers prepared sulfonated phenol and bisphenol A based HCPs and used them as reusable acid catalysts for esterification and transesterification with various vegetable oils and fatty acids. The synthesized sulfonated HCPs showed high catalytic activity at room temperature and higher temperature as well as outstanding recyclability.[30] Sulfonated hyper-cross-linked porous polyacetylene networks obtained from 1,3 and 1,4-diethynyl benzene (DEB) have been synthesized by a chain-growth homopolymerization

following by sulfonation. The parent materials showed high surface areas up to 1200 $m^2/g$, while upon sulfonation the surface areas decreased to 550 $m^2/g$ after. The sulfonated polyacetylene networks showed high %conversion of FFAs to FAME after refluxing for 24 h, however the reusability of the catalysts for biodiesel production was not reported.[36]

In this study we report the polymerization of bromophenol blue (BB) and bromocresol green (BG), which contain a sulfonate group, with alkyne monomers to produce BB and BG CMPs. The synthesized CMPs were post-synthetically modified via a sulfonation reaction to increase the acidity of the materials. The synthesized materials were used as acid catalysts for biodiesel production from various vegetable oils, waste oils and FFAs showing high catalytic activity at room temperature as well as excellent reusability.

## Experimental

***Materials.*** Bromophenol blue (BB), 1,3,5-triethynylbenzene (TEB) and copper (I) iodide (CuI) were obtained from Alfa Aesar. 1,4-diethynylbenzene (DEB), myristic acid and palmitic acid were purchased from Acros Organics. Oleic acid was obtained from Fluorochem. All other chemicals were purchased from Sigma Aldrich. Anhydrous *N*,*N*'-dimethyformamide (DMF) and triethylamine (TEA) were used for all polymer synthesis. All chemicals were used as received and had a purity over 95%. Widely available vegetable oils were purchased from supermarkets and used as received.

***Synthesis of BB and BG based CMPs via Sonogashira – Hagihara cross coupling.*** BB or BG (0.5 mmol), TEB (1 mmol) or DEB (1.5 mmol) and CuI (0.079 mmol) were added into a two-neck round bottom flask and it was degassed and backfilled with nitrogen gas 3 times. Anhydrous DMF (5 mL) and TEA (5 mL) were added and the reaction mixture was heated to 100 °C under nitrogen

atmosphere. Tetrakis(triphenylphosphine)palladium(0) (0.043 mmol) was mixed with 2 mL of anhydrous DMF and the mixture was injected as a slurry to the reaction. The reaction was left for 24 h. The solid product was filtered by vacuum filtration and washed with methanol, chloroform and acetone, respectively. The washed product was further purified by Soxhlet extraction using methanol for 16 h and the obtained solid was dried under vacuum at 80 °C. Yields were 120.1, 119.9, 98.8 and 113.5% for BB+TEB, BG+TEB, BB+DEB and BG+DEB, respectively.

***Sulfonation of BB and BG CMPs.*** Sulfonation reaction was conducted following the procedure as reported by Kalla *et al*.[30] 0.4 g of BB- or BG-CMP was suspended and stirred in dichloromethane (DCM). An excess of chlorosulfonic acid was used to ensure a high degree of sulfonation. A mixture of chlorosulfonic acid (4 mL) and 10 mL of DCM was slowly added into the polymer suspension and the reaction was stirred for 48 h at the room temperature. After that, the reaction mixture was diluted with 50 mL of DCM and was vacuum filtered and washed with water until the filtrate was neutral. The solid product was dried under vacuum at 80 °C. For comparison, BB- and BG-CMPs were also treated with hydrochloric acid using the same procedure.

**Characterization**

***Nitrogen gas adsorption and desorption isotherms.*** Nitrogen gas sorption isotherms were acquired by a Micromeritics ASAP 2020Plus analyzer using high purity gases at 77 K. All samples (ca. 0.1 g) were degassed at 120 °C under dynamic vacuum prior to analysis. Surface areas were calculated using Brunauer-Emmett-Teller (BET) theory over a relative pressure range of 0.01–0.15 $P/P_0$. Differential pore sizes were analyzed using the NL-DFT method.

***1D $^{1}H$–$^{13}C$ cross-polarization magic angle spinning (CP/MAS).*** The synthesized polymers were filled into 4 mm zirconia rotors before analyzed with a Bruker Avance III HD spectrometer at 125.76 MHz (500.13 MHz $^{1}H$) at a MAS rate of 10.0 kHz. The $^{1}H$ $\pi/2$ pulse was 3.4 μs, and two-pulse phase modulation (TPPM) decoupling was used during the acquisition. The Hartmann–Hahn condition was set using hexamethylbenzene. The spectra were measured using a contact time of 2.0 ms. The relaxation delay $D_1$ for each sample was individually determined from the proton $T_1$ measurement ($D_1 = 5 \times T_1$). Data was collected until sufficient signal-to-noise was obtained, typically greater than 256 scans. The chemical shift values are referred to that of TMS.

***$^{1}H$ NMR and $^{13}C$ Nuclear magnetic resonance (NMR) spectroscopy.*** Solution state NMR was perform using Bruker AV 400MHz. Samples were dissolved in deuterated chloroform and filtered by cotton wool prior analysis at room temperature.

***Fourier transform infrared (FT–IR) spectroscopy.*** FTIR was performed using a PerkinElmer Spectrum 100. Samples were analyzed with a diamond ATR accessory or were mixed with KBr and pressed into a disk before being measured in transmission mode.

***Elemental analysis (EA).*** EA was obtained using Elementar Vario MICRO Cube CHN/S analyzer by burning a sample in a stream of oxygen. Combustion products were passed through a copper tube to remove excess oxygen and reduce $NO_x$ to $N_2$ before separated with a Thermal Programmed Desorption column and detected by a thermal conductivity detector (TCD). Halogen analysis was performed using the Schöniger flask combustion method and a titration was used to determine the amount of required element.

***Thermogravimetric analysis (TGA).*** TGA was performed using PE Pyris. Approximately 5 mg of material was pyrolysed under nitrogen atmosphere from room temperature to 800 °C using 10 °C/min of heating rate.

***Esterification of free fatty acids (FFAs) and transesterification of different vegetable oils with methanol.*** The procedure was adapted from previous work.[30] Fatty acid (1 mmol), 10 mg of acid catalyst and 2 mL of methanol (50 mmol) were added into a reaction vessel and stirred at room temperature or 60 °C. The catalyst was doubled if dicarboxylic fatty acids were used. For transesterification, 100 mg of vegetable oil, various amounts of acid catalyst and 5.7 mL of methanol were mixed in a reaction flask and stirred at 60 °C for 24 h. The catalyst was filtered and washed with chloroform. The filtrate was evaporated under vacuum and the product was dried using vacuum oven at 60 °C. Yield of fatty acid methyl ester (FAME) and conversion of oil to FAME were calculated by $^1$H NMR by following equations[30,37];

$$Yield(\%)\ for\ esterification = \frac{I_{ME}}{I_{CH2}} \times 100$$

$$Yield(\%)\ for\ transesterification = \frac{2 \times I_{ME}}{3 \times I_{\alpha-CH2}} \times 100$$

$$Conversion(\%) = \frac{4 \times I_{ME}}{(4 \times I_{ME}) + (9 \times I_{TG})} \times 100$$

Where: $I_{ME}$ is the peak area of methyl ester protons at 3.6 ppm, $I_{CH2}$ is the peak area of methylene protons at 2.25 ppm, $I_{\alpha\text{-}CH2}$ is the peak area of α-carbonyl methylene protons at 2.3, and $I_{TG}$ is the peak area of glyceridic protons at 4.15 ppm

**Results and Discussion**

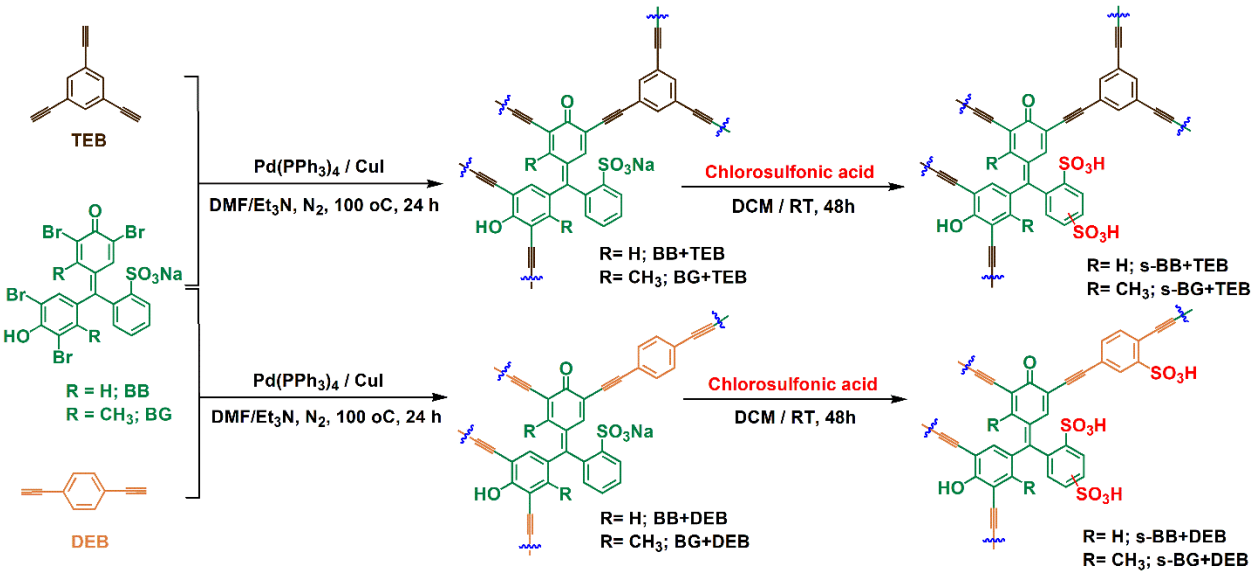


**Scheme 1.** Synthesis of BB and BG based CMPs via Sonogashira-Hagihara coupling and sulfonation of the synthesized CMPs.

## Characterization

The tetrabromo functional monomers bromophenol blue (BB) and bromocresol green (BG) were reacted with either 1,3,5-triethynelbenzene (TEB) or 1,4-diethynylbenzene (DEB) to yield CMPs BB+TEB, BB+DEB, BG+TEB and BG+DEB using a Sonogashira-Hagihara cross coupling reaction with $Pd(PPh_3)_4$ and CuI as catalysts in yields of 98.8-120.1% (Scheme 1). Yields greater than 100% are attributed to incomplete condensation of the monomers i.e. the presence of unreacted bromo end groups, and trapped solvents as is commonly reported for similar CMPs and POPs in general.[13,38,39] Indeed, the elemental analysis results confirmed the presence of halogens in the polymers as shown in Table S1. It is worth noting that it is difficult to locate the position of the sufonic groups in the sulfonated polymer networks, Scheme 1 demonstrates the possible positions of sulfonate groups on the polymer network.

The FT-IR spectra (Figure 1a) display a peak at 2362 $cm^{-1}$ assigned to internal alkyne linkages (–C≡C-) confirming that polymerization has occurred.[40] The absence of peaks at 457, 461 and 3278 $cm^{-1}$ corresponding to $C_{Ar}$-Br in BB and BG monomers as well as C-H in terminal alkyne of TEB and DEB monomers (Figure S1), respectively, confirmed that the monomers were successfully incorporated into the polymer networks. The peaks at 624, 1021, and 1174 $cm^{-1}$ correspond to C-S stretching, S=O symmetric and asymmetric stretching in -$SO_3H$.[31] After sulfonation, the intensity of these peaks increased due to the further incorporation of sulfonic groups into the polymer networks. Furthermore there is evidence of modification of the alcohol groups into sulfates (-$OSO_3H$) with O=S=O asymmetric and symmetric stretching peaks observed at 1220 and 1040 $cm^{-1}$, respectively, as well as the S-O stretching peak observed at 890 $cm^{-1}$.[30] The $^{13}C$ CP/MAS spectra of the as synthesized and sulfonated CMPs are shown in Figure 1(b). The peaks at 123, 129, 144, and 154 ppm are assigned to ($C_{Ar}$-H), ($C_{Ar}$-C), ($C_{Ar}$-$SO_3^-$), and ($C_{Ar}$-OH), respectively. The small peak at 100 ppm corresponds to alkyne linkages which further confirm the formation of a CMP network.[40] The spectra for BG CMPs show an additional peak at 16 ppm which corresponds to the methyl groups. After sulfonation, the intensity of the 123 ppm ($C_{Ar}$-H) peak decreases while the peak at 144 ppm ($C_{Ar}$-$SO_3^-$) increases due to the substitution of sulfonic acid groups on the aromatic ring. The broadening of peak at 154 ppm indicates the esterification

of the $C_{Ar}$-OH group to $C_{Ar}$-$OSO_3H$ which is consistent with the FTIR.

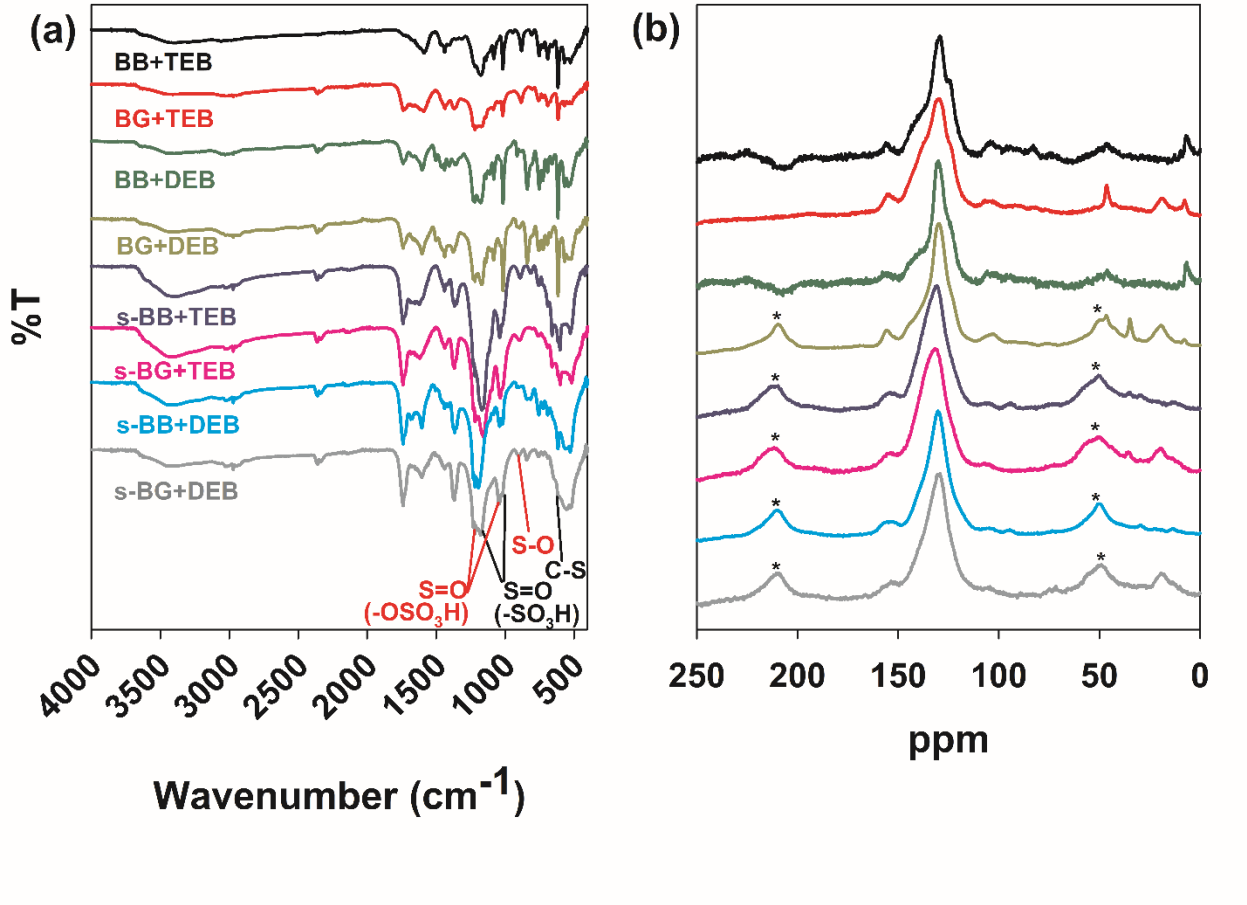


**Figure 1.** (a) IR and (b) $^{13}C$ CP/MAS spectra of the as-synthesized CMPs and sulfonated CMPs. (* denotes sideband spinning)

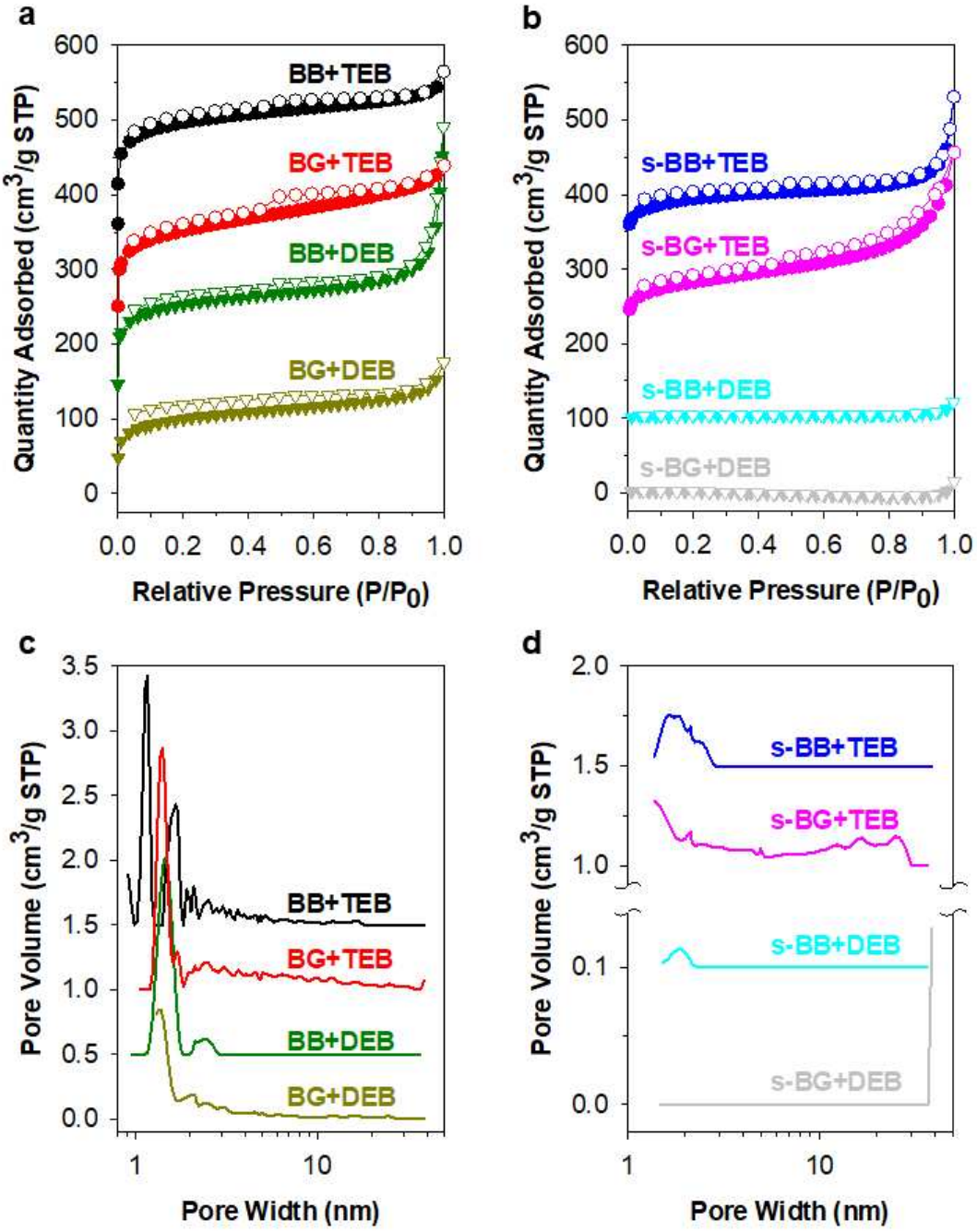


**Figure 2.** (a) Nitrogen gas sorption isotherms (filled is adsorption and emptied is desorption) of the synthesized CMPs and (b) the sulfonated CMPs, (c) pore size distribution of the synthesized CMPs and (d) the sulfonated CMPs. The isotherms were offset by 100 $cm^3/g$ and 0.5 $cm^3/g$ for pore size distribution.

**Table 1.** BET surface areas, total pore volumes, sulfur contents and acidity of the synthesized CMPs.

| Sample | $S_{BET}$ ($m^2/g$) | $V_t$ ($cm^3/g$) | S Content (%) | Acidity (mmol/g) |
|---|---|---|---|---|
| BB+TEB | 747 | 0.38 | 2.41 | 1.54 |
| BB+DEB | 580 | 0.35 | 2.75 | 1.55 |
| BG+TEB | 566 | 0.34 | 2.23 | 1.83 |
| BG+DEB | 373 | 0.22 | 2.34 | 1.89 |
| HCl-BB+TEB | 688 | 0.34 | 3.78 | 1.72 |
| HCl-BB+DEB | 511 | 0.26 | 3.31 | 1.69 |
| HCl-BG+TEB | 532 | 0.29 | 2.79 | 1.89 |
| HCl-BG+DEB | 463 | 0.27 | 2.73 | 1.84 |
| s-BB+TEB | 349 | 0.22 | 8.67 | 3.53 |
| s-BB+DEB | 12 | 0.01 | 10.24 | 7.67 |
| s-BG+TEB | 303 | 0.29 | 9.15 | 4.39 |
| s-BG+DEB | 60 | 0.003 | 9.11 | 4.04 |

The obtained materials exhibit type I $N_2$ isotherms with high BET surface areas ($S_{BET}$) from 373 to 747 $m^2/g$ and total pore volumes ($V_t$) between 0.22 and 0.38 $cm^3/g$ as shown in Table 1 and Figure 2(a). All synthesized CMPs show a narrow pore size distribution with the main peaks located at a pore width less than 2 nm confirming they are indeed microporous materials (Figure 2(b)). BG based CMPs showed lower surface areas than BB based CMPs due to steric hindrance from the adjacent methyl group resulting in lower conversion of monomers to polymer networks as confirmed by the higher bromine contents according to elemental analysis (Table S1). The polymers produced from TEB showed higher $S_{BET}$ than from DEB due to the higher connectivity

of the TEB monomer compared to the linear linker of DEB.[5,41–44] After sulfonation, the $S_{BET}$ and $V_t$ of all samples dropped dramatically due to the incorporation of sulfonic groups in the polymer networks. The DEB versions of the functionalized CMPs showed a lower $S_{BET}$ than those synthesized from TEB due to the greater sulfonic group substitution of the DEB than TEB resulting from less stearic hindrance. It is consistent with elemental analysis results (Table S1) that all sulfonated polymers showed higher sulfur content than non-functionalized and HCl treated CMPs and the DEB versions polymers possessed higher amount of sulfur than TEB ones. The halogen content displayed in Table S1 also increased after treated with both HCl and chlorsulfonic acids probably due to the interference of residual chlorine.[45] The acidity of the synthesized CMPs was been determined by reacting with aqueous NaOH and then back titrating with HCl aqueous solution as described in previous works[29,30]. The acidity of the polymers were in agreement with elemental analysis results and were in the range of 1.54 to 7.67 mmol/g, which exceeds that of previously reported microporous polymers.[29–31,36]All samples were analyzed by TGA under nitrogen atmosphere as shown in Figure S4. All synthesized CMPs had high thermal stability with decomposition temperature from 200 to 300 °C. BB based CMPs showed higher degradation temperature (ca. 300 °C) than the BG based CMPs (ca. 250 °C) due to the loss of methyl group in the BG based polymers. All sulfonated CMPs showed lower degradation temperature at approximately 200 °C due to the loss of sulfonic group in the materials which is consistent with the literature.[36]

**Esterification of FFAs and Transesterification of Vegetable Oils Using the Acid Catalysts.**

The synthesized catalysts were used for the esterification of various chain lengths ($\mathbf{C_6 - C_{18}}$) of mono and dicarboxylic FFAs such as myristic, palmitic, stearic, oleic, adipic and sebacic acids. The no catalyst and non-functionalized CMPs showed very low %yield of the FAME product at

60 °C for 24 h due to the absence of an acid catalyst and the lack of acidity of the materials, respectively (Entry1-5). The HCl treated CMPs (Entry 6-9, 14-17) showed low to moderate % yield while the sulfonated CMPs (Entry 10-13) showed a high % yield of methyl ester product of lauric acid up to 94% because the sulfonated catalysts possessed more sulfonic groups in the polymer networks as shown in Table 2. s-BB+TEB, the lowest acidity sulfonated catalyst showed a high %yield which is similar to other sulfonated polymers, so it indicated that the acidity of s-BB+TEB was high enough to catalyze the esterification of FFAs. The catalytic activity was likely independent on the surface areas of the polymers as all polymers showed similar %yield.

**Table 2.** Esterification of FFAs using the synthesized CMPs

| **Entry** | **Fatty acid** | **Catalyst** | **Temp (°C)** | **Time (h)** | **Yield (%)** |
|---|---|---|---|---|---|
| 1 | Lauric acid | No catalyst | 60 | 24 | 2.6 |
| 2 | Lauric acid | BB+TEB | 60 | 24 | 2.7 |
| 3 | Lauric acid | BB+DEB | 60 | 24 | 2.2 |
| 4 | Lauric acid | BG+TEB | 60 | 24 | 4.3 |
| 5 | Lauric acid | BG+DEB | 60 | 24 | 1.9 |
| 6 | Lauric acid | HCl-BB+TEB | 60 | 24 | 16.2 |
| 7 | Lauric acid | HCl-BB+DEB | 60 | 24 | 64.2 |
| 8 | Lauric acid | HCl-BG+TEB | 60 | 24 | 75.3 |
| 9 | Lauric acid | HCl-BG+DEB | 60 | 24 | 15.1 |
| 10 | Lauric acid | s-BB+TEB | 60 | 24 | 93.7 |
| 11 | Lauric acid | s-BB+DEB | 60 | 24 | 89.3 |
| 12 | Lauric acid | s-BG+TEB | 60 | 24 | 92.6 |
| 13 | Lauric acid | s-BG+DEB | 60 | 24 | 93.6 |
| 14 | Myristic acid | HCl-BB+TEB | 60 | 24 | 24.0 |

| | | | | | |
|---|---|---|---|---|---|
| 15 | Myristic acid | HCl-BB+DEB | 60 | 24 | 63.5 |
| 16 | Myristic acid | HCl-BG+TEB | 60 | 24 | 66.7 |
| 17 | Myristic acid | HCl-BG+DEB | 60 | 24 | 77.9 |
| 18 | Adipic acid | s-BB+DEB | 60 | 6 | 91.3 (91.3)* |
| 19 | Sebacic acid | s-BB+DEB | 60 | 6 | 95.2 (92.6)* |

Reaction condition: 1mmol of FFA, 2 mL of methanol and 10 mg of catalyst was used for monocarboxylic acid and the catalyst was doubled for dicarboxylic acid.

* The number in brackets is %yield when 10 mg of the catalyst was used.

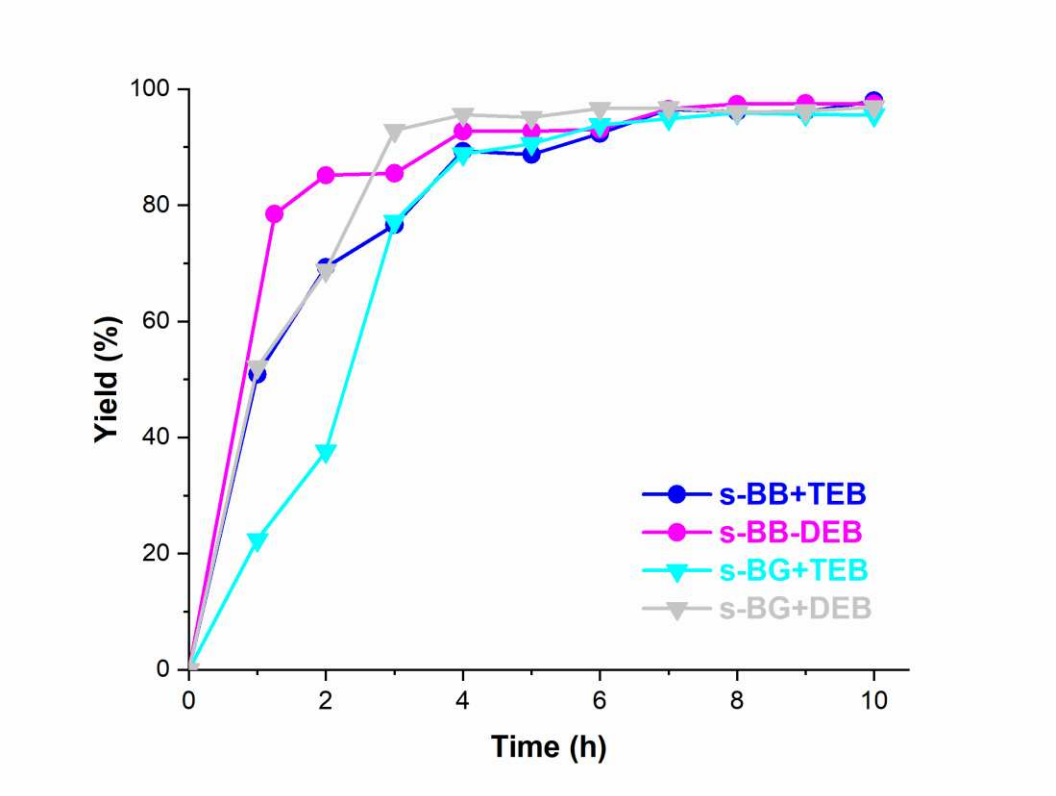


**Figure 3.** Kinetic studies of esterification of myristic acid with 2 mL of methanol using 10 mg of different sulfonated CMPs at 60 °C.

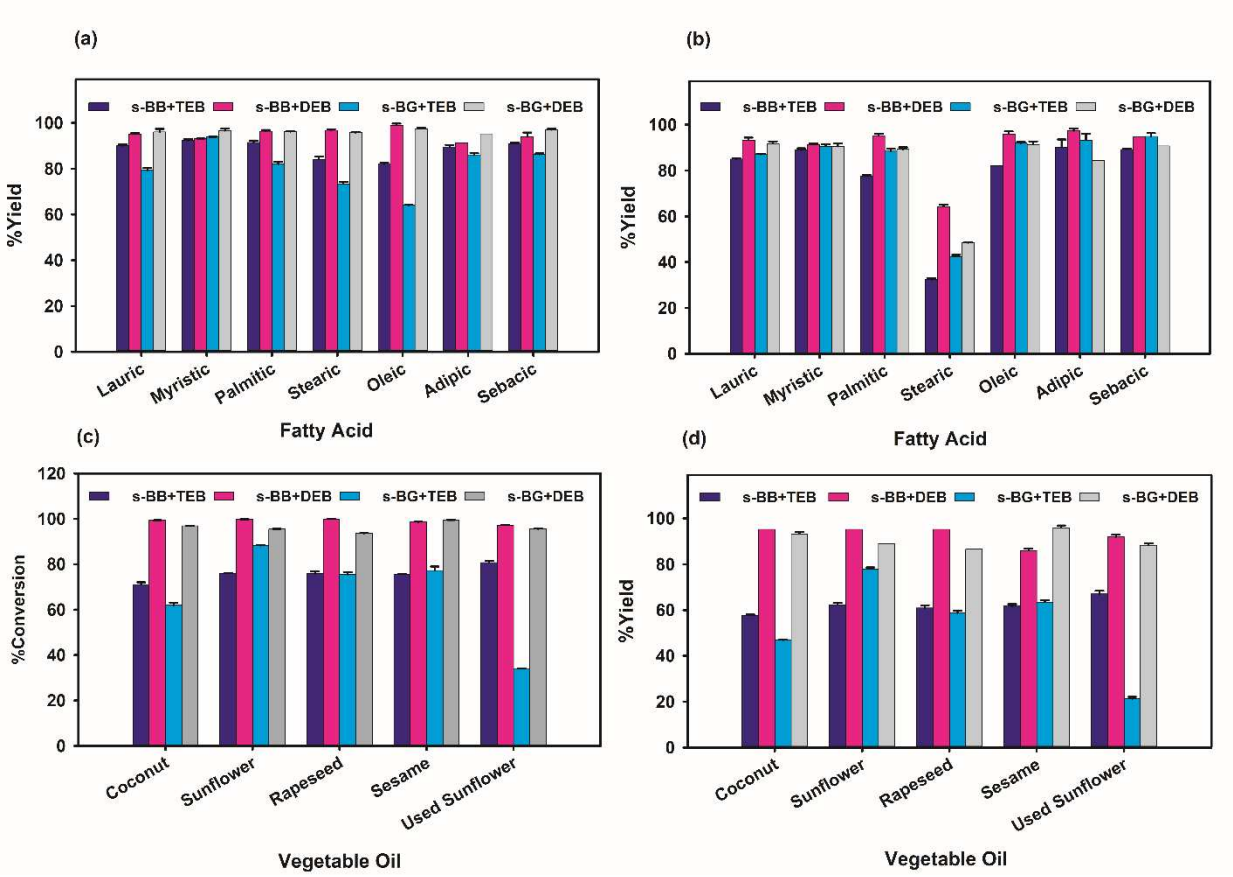


**Figure 4.** (a) Esterification of FFAs at 60 °C for 6 h, (b) esterification of FFAs at 25 °C for 24 h, (c) %conversion of transesterification of vegetable oils and (d) %yield of transesterification of vegetable oils at 60 °C for 24 h using different sulfonated polymers. Esterification: 1 mmol of FFAs, 2 mL of methanol, 10 mg of catalyst was used for monocarboxylic acid and the amount of catalyst was double when dicarboxylic was used. Transesterification: 100 mg of oil, 5.7 mL of methanol and 60 mg of catalyst was used.

The catalytic activity of different sulfonated CMPs on esterification of myristic acid at 60 °C was studied at different reaction times (Figure 3). The results illustrate that s-BB+DEB achieved the highest yield of 85.5% after 2 h while s-BB+TEB, s-BG+TEB and s-BG+DEB showed lower % yields of 69.5, 37.3 and 69.2, respectively. The s-BB+DEB showed the highest activity at the beginning of the reaction due to the highest acidity of the catalyst. The %yields of product

continuously increased after 2 h and %yields reached a plateau after 3h for s-BG+DEB, 4h for s-BB+DEB and 6 h for the rest of sulfonated polymers. All sulfonated catalysts showed a high yield of products for various FFAs at 60 °C for 6 h i.e., 82-92% for s-BB+TEB, 91-99% for s-BB+DEB, 64-94% for s-BG+TEB, and 95-97% for s-BG+DEB as shown in Figure 4(a). Moreover, the sulfonated catalysts also showed very high yields of biodiesel products up to 90, 97, 95 and 92% for s-BB+TEB, s-BB+DEB, s-BG+TEB and s-BG+DEB, respectively even at room temperature for 24 h for different FFAs as illustrated in Figure 4(b). Stearic acid, which has the longest chain FFA in this study, was partially soluble in methanol at room temperature leading to a relatively low % yield of 31.8-64.9 % which increased to 74.0-97.1 % at 60 °C due to the better solubility of stearic acid at the higher temperature. From the previous work, the catalyst was doubled to 20 mg when dicarboxylic acids were used.[29,30] It is worth noting that s-BB+DEB showed a very high yield of 91.3 and 92.6 % for dicarboxylic acids; adipic and sebacic acids, respectively, when 10 mg of the catalyst was used at 60 °C for 6 h as shown in Table 2 (Entry 18-19). This indicates that the synthesized catalysts still showed excellent catalytic activity even at a lower amount of catalyst loading. The results suggest that sulfonated materials synthesized in this work have similarly high catalytic activity for esterification of FFAs at either room temperature or 60 °C compared with the previous reported sulfonated HCPs and CMPs[29–31,36]. Sulfonated phenol and bisphenol A based HCPs showed high %yield of 78.5-96.6% for esterification of different FFAs at room temperature from 6-24 h.[30] Sulfonated carbazole based HCPs also showed high %yield of 93-99% at room temperature using 0.5 mmol of FFA and 6 mg of catalysts.[29] Sulfonated pyrene based HCPs gave high %yield of 88-94% for esterification of FFAs at room temperature for 10h, but higher amount of catalysts (17-25 mg) was required for 1 mmol of FFA.[31] Sulfonated hyper-cross-linked porous

polyacetylene yielded up to 99% of FAME synthesized from various FFAs using 1%wt of catalyst. However, they needed higher temperature and longer time (60 °C for 24h).[36]

Different vegetable oils such as coconut, sunflower, rapeseed and sesame were selected to react with methanol using different synthesized CMP catalysts via transesterification. Likewise, the non-functionalized and HCl treated CMPs (Entries 1-8) showed much lower conversion than the sulfonated CMPs (Entries 9, 16, 24-25, 26-29) as shown in Table 3. The effect of the amount of catalyst was also studied using s-BB+TEB and s-BB+DEB catalysts for transesterification of coconut oil at 60 °C for 24 h. The results showed that an increase in amount of the catalysts led to a higher conversion of triglycerides to biodiesel products, but the conversions reached a plateau after 60 mg for both catalysts, thus 60 mg of catalyst was the optimum amount of the catalyst as illustrated in Table 3 (Entries 9-15, 16-22). The sulfonated catalysts showed the high conversions of tranesterification of various vegetable oils up to 81, 100, 88 and 99% and high yields up to 67, 95, 78, 96% for s-BB+TEB, s-BB+DEB, s-BG+TEB and s-BG+DEB, respectively due to the high acidity of the catalysts as shown in Figure 4(c) and (d). However, the % conversion of coconut oil to the products using s-BB+DEB as a catalyst decreased dramatically to 23.2 % at room temperature (Table 3, Entry 23), which is consistent with the previous reports[30,31], so a higher temperature is needed in order to increase a speed of molecules and therefore a higher kinetic rate.[46] Moreover, the sulfonated polymers also exhibited a very high conversion up to 97.1 % for waste cooking sunflower oil. This indicates that our synthesized catalysts have potential to be used for the production of biodiesel from waste cooking oils, which not only reduces the use of fossil fuel and carbon emissions, but also prevents pollution caused by the waste cooking oils.

**Table 3.** Transesterification of various vegetable oils using the synthesized CMPs

| Entry | Oil | Catalyst | Catalyst amount (mg) | %Conversion |
|---|---|---|---|---|
| 1 | Coconut | BB+TEB | 10 | 0.9 |
| 2 | Coconut | BB+DEB | 10 | 0.0 |
| 3 | Coconut | BG+TEB | 10 | 0.9 |
| 4 | Coconut | BG+DEB | 10 | 0.4 |
| 5 | Coconut | HCl-BB+TEB | 10 | 0.0 |
| 6 | Coconut | HCl-BB+DEB | 10 | 0.9 |
| 7 | Coconut | HCl-BG+TEB | 10 | 1.3 |
| 8 | Coconut | HCl-BG+DEB | 10 | 0.9 |
| 9 | Coconut | s-BB+TEB | 10 | 12.3 |
| 10 | Coconut | s-BB+TEB | 20 | 25.2 |
| 11 | Coconut | s-BB+TEB | 30 | 47.2 |
| 12 | Coconut | s-BB+TEB | 40 | 52.3 |
| 13 | Coconut | s-BB+TEB | 50 | 57.9 |
| 14 | Coconut | s-BB+TEB | 60 | 71.8 |
| 15 | Coconut | s-BB+TEB | 70 | 68.5 |
| 16 | Coconut | s-BB+DEB | 10 | 49.0 |
| 17 | Coconut | s-BB+DEB | 20 | 73.2 |
| 18 | Coconut | s-BB+DEB | 30 | 88.4 |
| 19 | Coconut | s-BB+DEB | 40 | 95.4 |
| 20 | Coconut | s-BB+DEB | 50 | 97.0 |
| 21 | Coconut | s-BB+DEB | 60 | 99.4 |
| 22 | Coconut | s-BB+DEB | 70 | 99.4 |
| 23 | Coconut | s-BB+DEB | 60 | 23.2* |
| 24 | Coconut | s-BG+TEB | 10 | 30.3 |
| 25 | Coconut | s-BG+DEB | 10 | 47.9 |

| | | | | |
|---|---|---|---|---|
| 26 | Sunflower | s-BB+TEB | 10 | 20.2 |
| 27 | Sunflower | s-BB+DEB | 10 | 22.7 |
| 28 | Sunflower | s-BG+TEB | 10 | 18.8 |
| 29 | Sunflower | s-BG+DEB | 10 | 35.5 |

The transesterification was performed at 60 °C for 24 h using 100 mg of oil and 5.7 mL of methanol.

*The reaction temperature was 25 °C.

**Reusability Testing**

s-BB+DEB was selected for reusability testing due to having the highest acidity and high catalytic activity (Figure 5). The esterification of myristic acid was performed at 60 °C for 6 h using 10 mg of the catalyst. The catalyst was washed after the reaction with excessive chloroform and dried in a vacuum oven at 60 °C. The same amount of catalyst (10 mg) was used in each cycles. The catalyst showed good stability with just around 10% activity loss after the 4th cycle. The slight loss of activity might cause by the pore blocking by FFA and its product and the loss of acid sites over multiple uses as sulfur content decreased to 4.16% according to elemental analysis (Table S1)[47] TGA (Figure S4) of the used catalyst showed a small decrease of %residual of the material when it was compared with the fresh catalyst indicative of the high thermal stability of the catalyst. FTIR spectra (Figure S5) show that s-BB+DEB still possesses sulfonic groups after being reused.

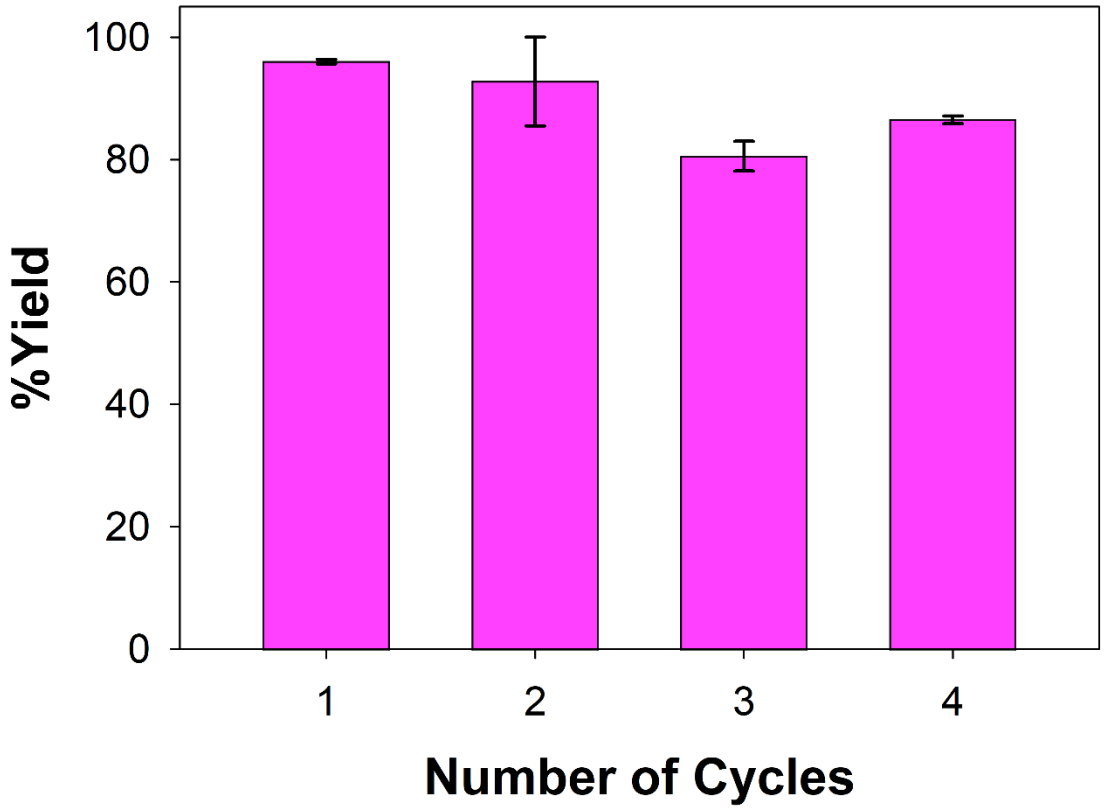


**Figure 5.** Reusability study of esterification of myristic acid (1 mmol) using 2 mL of methanol and 10 mg of s-BB+DEB at 60 °C for 6 h.

## Conclusions

BB and BG containing CMPs were successfully synthesized using Songogashira-Hagihara coupling to produce highly porous materials. The sulfonated BB and BG CMPs showed high acidity which resulted in high activity toward esterification of FFAs and transesterification of various vegetable oils and waste cooking oil. The functionalized CMPs show excellent stability and can be reused over 4 cycles, and this acid functionalized CMPs shows great potential to be a recyclable catalyst for biodiesel production from waste cooking oil, which is one of the greenest alternative fuel to replace fossil diesel.

**Corresponding Author**

*Dr Robert Dawson, Department of Chemistry, University of Sheffield. Sheffield S3 7HF, United Kingdom r.dawson@sheffield.ac.uk

**Funding Sources**

We would like to thank the Development and Promotion of Science and Technology Talents Project (DPST), Royal Government of Thailand scholarship for PhD funding and financial support for this project.

**Supporting Information**.

Supporting information is available free of charge at http://pubs.acs.org

Associated content: Figure S1. IR spectra of the monomers, Figure S2. IR spectra of HCl treated CMPs, Figure S3. Nitrogen sorption isotherms and pore size distributions of HCl treated CMPs, Determination of acidity of the synthesized polymers. Table S1 Elemental analysis of the synthesized polymers. Figure S4. TGA graphs of the synthesized CMPs, Figure S5. FTIR spectra of fresh and reused s-BB+DEB, Figure S6-S29. $^{1}$H NMR spectra of FFAs, oils, and biodiesel products.

**References**

(1) Budd, P. M.; Msayib, K. J.; Tattershall, C. E.; Ghanem, B. S.; Reynolds, K. J.; McKeown, N. B.; Fritsch, D. Gas Separation Membranes from Polymers of Intrinsic Microporosity. *J. Memb. Sci.* **2005**, *251* (1–2), 263–269. https://doi.org/10.1016/j.memsci.2005.01.009.

(2) Dai, Y.; Li, W.; Chen, Z.; Zhu, X.; Liu, J.; Zhao, R.; Wright, D. S.; Noori, A.; Mousavi, M. F.; Zhang, C. An Air-Stable Electrochromic Conjugated Microporous Polymer as an

Emerging Electrode Material for Hybrid Energy Storage Systems. *J. Mater. Chem. A* **2019**, *7* (27), 16397–16405. https://doi.org/10.1039/c9ta03001h.

(3) Zhou, Y.-B.; Zhan, Z.-P. Conjugated Microporous Polymers for Heterogeneous Catalysis. *Chem. - An Asian J.* **2018**, *13* (1), 9–19. https://doi.org/10.1002/asia.201701107.

(4) Jiang, J. X.; Li, Y.; Wu, X.; Xiao, J.; Adams, D. J.; Cooper, A. I. Conjugated Microporous Polymers with Rose Bengal Dye for Highly Efficient Heterogeneous Organo-Photocatalysis. *Macromolecules* **2013**, *46* (22), 8779–8783. https://doi.org/10.1021/ma402104h.

(5) Wang, C. A.; Li, Y. W.; Cheng, X. L.; Zhang, J. P.; Han, Y. F. Eosin Y Dye-Based Porous Organic Polymers for Highly Efficient Heterogeneous Photocatalytic Dehydrogenative Coupling Reaction. *RSC Adv.* **2017**, *7* (1), 408–414. https://doi.org/10.1039/c6ra25123d.

(6) Kang, C. W.; Lee, D. H.; Shin, Y. J.; Choi, J.; Ko, Y. J.; Lee, S. M.; Kim, H. J.; Ko, K. C.; Son, S. U. Conjugated Macro-Microporous Polymer Films Bearing Tetraphenylethylenes for the Enhanced Sensing of Nitrotoluenes. *J. Mater. Chem. A* **2018**, *6* (36), 17312–17317. https://doi.org/10.1039/c8ta06744a.

(7) James, A. M.; Derry, M. J.; Train, J. S.; Dawson, R. Dispersible Microporous Diblock Copolymer Nanoparticles via Polymerisation-Induced Self-Assembly. *Polym. Chem.* **2019**, *10* (28), 3879–3886. https://doi.org/10.1039/c9py00596j.

(8) Zhao, Y.; Ma, W.; Xu, Y.; Zhang, C.; Wang, Q.; Yang, T.; Gao, X.; Wang, F.; Yan, C.; Jiang, J.-X. Effect of Linking Pattern of Dibenzothiophene- *S* , *S* -Dioxide-Containing Conjugated Microporous Polymers on the Photocatalytic Performance. *Macromolecules*

**2018**, *51* (23), 9502–9508. https://doi.org/10.1021/acs.macromol.8b02023.

(9) Yan, X.; Liu, H.; Li, Y.; Chen, W.; Zhang, T.; Zhao, Z.; Xing, G.; Chen, L. Ultrastable Covalent Organic Frameworks via Self-Polycondensation of an A2B2 Monomer for Heterogeneous Photocatalysis. *Macromolecules* **2019**, *52* (21), 7977–7983. https://doi.org/10.1021/acs.macromol.9b01600.

(10) Cote, A. P.; Benin, A. I.; Ockwig, N. W.; O'Keeffe, M.; Matzger, A. J.; Yaghi, O. M. Porous, Crystalline, Covalent Organic Frameworks. *Science (80-. ).* **2005**, *310* (5751), 1166–1170.

(11) Tan, L.; Tan, B. Hypercrosslinked Porous Polymer Materials: Design, Synthesis, and Applications. *Chemical Society Reviews*. Royal Society of Chemistry June 7, 2017, pp 3322–3356. https://doi.org/10.1039/c6cs00851h.

(12) Jiang, J. X.; Su, F.; Trewin, A.; Wood, C. D.; Campbell, N. L.; Niu, H.; Dickinson, C.; Ganin, A. Y.; Rosseinsky, M. J.; Khimyak, Y. Z.; Cooper, A. I. Conjugated Microporous Poly (Aryleneethynylene) Networks. *Angew. Chemie-International Ed.* **2007**, *46* (45), 8574–8578. https://doi.org/10.1002/anie.200701595.

(13) Dawson, R.; Laybourn, A.; Clowes, R.; Khimyak, Y. Z.; Adams, D. J.; Cooper, A. I. Functionalized Conjugated Microporous Polymers. *Macromolecules* **2009**, *42* (22), 8809–8816. https://doi.org/10.1021/ma901801s.

(14) Jiang, J. X.; Trewin, A.; Adams, D. J.; Cooper, A. I. Band Gap Engineering in Fluorescent Conjugated Microporous Polymers. *Chem. Sci.* **2011**, *2* (9), 1777–1781. https://doi.org/10.1039/c1sc00329a.

(15) Sprick, R. S.; Bonillo, B.; Clowes, R.; Guiglion, P.; Brownbill, N. J.; Slater, B. J.; Blanc, F.; Zwijnenburg, M. A.; Adams, D. J.; Cooper, A. I. Visible-Light-Driven Hydrogen Evolution Using Planarized Conjugated Polymer Photocatalysts. *Angew. Chemie Int. Ed.* **2016**, *55* (5), 1792–1796. https://doi.org/10.1002/anie.201510542.

(16) Wang, B.; Xie, Z.; Li, Y.; Yang, Z.; Chen, L. Dual-Functional Conjugated Nanoporous Polymers for Efficient Organic Pollutants Treatment in Water: A Synergistic Strategy of Adsorption and Photocatalysis. *Macromolecules* **2018**, *51* (9), 3443–3449. https://doi.org/10.1021/acs.macromol.8b00669.

(17) Li, M.; Zhao, H.; Lu, Z. Y. Porphyrin-Based Porous Organic Polymer, Py-POP, as a Multifunctional Platform for Efficient Selective Adsorption and Photocatalytic Degradation of Cationic Dyes. *Microporous Mesoporous Mater.* **2020**, *292*, 109774. https://doi.org/10.1016/j.micromeso.2019.109774.

(18) Zhang, H.; Li, H.; Xu, C. C.; Yang, S. Heterogeneously Chemo/Enzyme-Functionalized Porous Polymeric Catalysts of High-Performance for Efficient Biodiesel Production. *ACS Catalysis*. American Chemical Society 2019, pp 10990–11029. https://doi.org/10.1021/acscatal.9b02748.

(19) Wang, M.; Ma, J.; Liu, H.; Luo, N.; Zhao, Z.; Wang, F. Sustainable Productions of Organic Acids and Their Derivatives from Biomass via Selective Oxidative Cleavage of C-C Bond. *ACS Catal.* **2018**, *8* (3), 2129–2165. https://doi.org/10.1021/acscatal.7b03790.

(20) Renewable fuel statistics 2019: Second provisional report - GOV.UK.

(21) Nasrollahzadeh, M.; Sajjadi, M.; Shokouhimehr, M.; Varma, R. S. Recent Developments in

Palladium (Nano)Catalysts Supported on Polymers for Selective and Sustainable Oxidation Processes. *Coordination Chemistry Reviews*. Elsevier B.V. October 15, 2019, pp 54–75. https://doi.org/10.1016/j.ccr.2019.06.010.

(22) Nasrollahzadeh, M.; Shafiei, N.; Nezafat, Z.; Bidgoli, N. S. S. Recent Progresses in the Application of Lignin Derived (Nano)Catalysts in Oxidation Reactions. *Molecular Catalysis*. Elsevier B.V. June 1, 2020, p 110942. https://doi.org/10.1016/j.mcat.2020.110942.

(23) Nasrollahzadeh, M.; Nezafat, Z.; Bidgoli, N. S. S.; Shafiei, N. Recent Progresses in Polymer Supported Cobalt Complexes/Nanoparticles for Sustainable and Selective Oxidation Reactions. *Molecular Catalysis*. Elsevier B.V. March 1, 2020, p 110775. https://doi.org/10.1016/j.mcat.2020.110775.

(24) Nasrollahzadeh, M.; Shafiei, N.; Nezafat, Z.; Soheili Bidgoli, N. S.; Soleimani, F. Recent Progresses in the Application of Cellulose, Starch, Alginate, Gum, Pectin, Chitin and Chitosan Based (Nano)Catalysts in Sustainable and Selective Oxidation Reactions: A Review. *Carbohydrate Polymers*. Elsevier Ltd August 1, 2020, p 116353. https://doi.org/10.1016/j.carbpol.2020.116353.

(25) Nasrollahzadeh, M.; Motahharifar, N.; Ghorbannezhad, F.; Soheili Bidgoli, N. S.; Baran, T.; Varma, R. S. Recent Advances in Polymer Supported Palladium Complexes as (Nano)Catalysts for Sonogashira Coupling Reaction. *Molecular Catalysis*. Elsevier B.V. January 1, 2020, p 110645. https://doi.org/10.1016/j.mcat.2019.110645.

(26) Du, M.; Agrawal, A. M.; Chakraborty, S.; Garibay, S. J.; Limvorapitux, R.; Choi, B.;

Madrahimov, S. T.; Nguyen, S. T. Matching the Activity of Homogeneous Sulfonic Acids: The Fructose-to-HMF Conversion Catalyzed by Hierarchically Porous Sulfonic-Acid-Functionalized Porous Organic Polymer (POP) Catalysts. *ACS Sustain. Chem. Eng.* **2019**, *7* (9), 8126–8135. https://doi.org/10.1021/acssuschemeng.8b05720.

(27) Xu, C.; Nasrollahzadeh, M.; Selva, M.; Issaabadi, Z.; Luque, R. Waste-to-Wealth: Biowaste Valorization into Valuable Bio(Nano)Materials. *Chemical Society Reviews*. Royal Society of Chemistry September 21, 2019, pp 4791–4822. https://doi.org/10.1039/c8cs00543e.

(28) Xu, C.; Nasrollahzadeh, M.; Sajjadi, M.; Maham, M.; Luque, R.; Puente-Santiago, A. R. Benign-by-Design Nature-Inspired Nanosystems in Biofuels Production and Catalytic Applications. *Renew. Sustain. Energy Rev.* **2019**, *112*, 195–252. https://doi.org/10.1016/j.rser.2019.03.062.

(29) Bhunia, S.; Banerjee, B.; Bhaumik, A. A New Hypercrosslinked Supermicroporous Polymer, with Scope for Sulfonation, and Its Catalytic Potential for the Efficient Synthesis of Biodiesel at Room Temperature. *Chem. Commun.* **2015**, *51* (24), 5020–5023. https://doi.org/10.1039/c4cc09872b.

(30) Kalla, R. M. N.; Kim, M.-R.; Kim, I. Sulfonic Acid-Functionalized, Hyper-Cross-Linked Porous Polyphenols as Recyclable Solid Acid Catalysts for Esterification and Transesterification Reactions. *Ind. Eng. Chem. Res.* **2018**, *57* (34), 11583–11591. https://doi.org/10.1021/acs.iecr.8b02418.

(31) Kundu, S. K.; Bhaumik, A. Pyrene-Based Porous Organic Polymers as Efficient Catalytic Support for the Synthesis of Biodiesels at Room Temperature. *ACS Sustain. Chem. Eng.*

**2015**, *3* (8), 1715–1723. https://doi.org/10.1021/acssuschemeng.5b00238.

(32) Gomes, R.; Bhanja, P.; Bhaumik, A. Sulfonated Porous Organic Polymer as a Highly Efficient Catalyst for the Synthesis of Biodiesel at Room Temperature. *J. Mol. Catal. A Chem.* **2016**, *411*, 110–116. https://doi.org/10.1016/j.molcata.2015.10.016.

(33) Guadalupe, J.; Ray, A. M.; Maya, E. M.; Gómez-Lor, B.; Iglesias, M. Truxene-Based Porous Polymers: From Synthesis to Catalytic Activity. *Polym. Chem.* **2018**, *9* (36), 4585–4595. https://doi.org/10.1039/c8py01082j.

(34) Kalla, R. M. N.; Reddy, S. S.; Kim, I. Acylation of Phenols, Alcohols, Thiols, Amines and Aldehydes Using Sulfonic Acid Functionalized Hyper-Cross-Linked Poly(2-Naphthol) as a Solid Acid Catalyst. *Catal. Letters* **2019**, *149* (10), 2696–2705. https://doi.org/10.1007/s10562-019-02811-w.

(35) Fu, J.; Chen, L.; Lv, P.; Yang, L.; Yuan, Z. Free Fatty Acids Esterification for Biodiesel Production Using Self-Synthesized Macroporous Cation Exchange Resin as Solid Acid Catalyst. *Fuel* **2015**, *154*, 1–8. https://doi.org/10.1016/j.fuel.2015.03.048.

(36) Sekerová, L.; Březinová, P.; Do, T. T.; Vyskočilová, E.; Krupka, J.; Červený, L.; Havelková, L.; Bashta, B.; Sedláček, J. Sulfonated Hyper-cross-linked Porous Polyacetylene Networks as Versatile Heterogeneous Acid Catalysts. *ChemCatChem* **2020**, *12* (4), 1075–1084. https://doi.org/10.1002/cctc.201901815.

(37) Naureen, R.; Tariq, M.; Yusoff, I.; Chowdhury, A. J. K.; Ashraf, M. A. Synthesis, Spectroscopic and Chromatographic Studies of Sunflower Oil Biodiesel Using Optimized Base Catalyzed Methanolysis. *Saudi J. Biol. Sci.* **2014**, *22* (3), 332–339.

https://doi.org/10.1016/j.sjbs.2014.11.017.

(38) Laybourn, A.; Dawson, R.; Clowes, R.; Hasell, T.; Cooper, A. I.; Khimyak, Y. Z.; Adams, D. J. Network Formation Mechanisms in Conjugated Microporous Polymers. *Polym. Chem.* **2014**, *5* (21), 6325–6333. https://doi.org/10.1039/C4PY00647J.

(39) Dawson, R.; Laybourn, A.; Khimyak, Y. Z.; Adams, D. J.; Cooper, A. I. High Surface Area Conjugated Microporous Polymers: The Importance of Reaction Solvent Choice. *Macromolecules* **2010**, *43*, 8524–8530. https://doi.org/10.1021/ma101541h.

(40) Geng, T. M.; Ye, S. N.; Wang, Y.; Zhu, H.; Wang, X.; Liu, X. Conjugated Microporous Polymers-Based Fluorescein for Fluorescence Detection of 2,4,6-Trinitrophenol. *Talanta* **2017**, *165*, 282–288. https://doi.org/10.1016/j.talanta.2016.12.046.

(41) Jiang, J. X.; Li, Y.; Wu, X.; Xiao, J.; Adams, D. J.; Cooper, A. I. Conjugated Microporous Polymers with Rose Bengal Dye for Highly Efficient Heterogeneous Organo-Photocatalysis. *Macromolecules* **2013**, *46* (22), 8779–8783. https://doi.org/10.1021/ma402104h.

(42) Wang, J.; Yang, H.; Jiang, L.; Liu, S.; Hao, Z.; Cheng, J.; Ouyang, G. Highly Efficient Removal of Organic Pollutants by Ultrahigh-Surface-Area-Ethynylbenzene-Based Conjugated Microporous Polymers: Via Adsorption-Photocatalysis Synergy. *Catal. Sci. Technol.* **2018**, *8* (19), 5024–5033. https://doi.org/10.1039/c8cy01379a.

(43) Xu, Y.; Jiang, D. Structural Insights into the Functional Origin of Conjugated Microporous Polymers: Geometry-Management of Porosity and Electronic Properties. *Chem. Commun.* **2014**, *50* (21), 2781–2783. https://doi.org/10.1039/c3cc49669d.

(44) Xu, Y.; Mao, N.; Feng, S.; Zhang, C.; Wang, F.; Chen, Y.; Zeng, J.; Jiang, J.-X. Perylene-Containing Conjugated Microporous Polymers for Photocatalytic Hydrogen Evolution. *Macromol. Chem. Phys.* **2017**, *218* (14), 1700049. https://doi.org/10.1002/macp.201700049.

(45) Wang, C. Y.; Tarter, J. G. Determination of Halogens in Organic Compounds by Ion Chromatography after Sodium Fusion. *Anal. Chem.* **1983**, *55* (11), 1775–1778. https://doi.org/10.1021/ac00261a029.

(46) C., A. E.; I., N. G.; C., E. C.; R., N. N. Effect of Reaction Temperature on the Yield of Biodiesel From Neem Seed Oil. *http://www.openscienceonline.com/* **2016**, *3* (3), 16. https://doi.org/7450147.

(47) Dantas, J.; Leal, E.; Cornejo, D. R.; Kiminami, R. H. G. A.; Costa, A. C. F. M. Biodiesel Production Evaluating the Use and Reuse of Magnetic Nanocatalysts Ni0.5Zn0.5Fe2O4 Synthesized in Pilot-Scale. *Arab. J. Chem.* **2020**, *13* (1), 3026–3042. https://doi.org/10.1016/j.arabjc.2018.08.012.